

Cytosolic Processing of Proteasomal Cleavage Products Can Enhance the Presentation Efficiency of MHC-1 Epitopes

Sascha Bulik

sascha@comets.de

Björn Peters

bjoern.peters@gmx.net

Christian Ebeling

h04442fv@rz.hu-berlin.de

Hergo Holzhütter

hergo@charite.de

Medical School (Charité), Institute of Biochemistry, Humboldt-University Berlin,
Monbijoustr. 2, D-10117 Berlin

Abstract

The vertebrate immune system is able to detect abnormal body cells by the specific repertoire of 8 – 12 residues long peptides (= epitopes or peptide antigens) presented at the cell surface by the MHC-1 molecule complex. The generation of an epitope starts with the degradation of endogenous proteins into primary oligomeric fragments by cytosolic proteases, predominantly the proteasome. These primary fragments may be further attacked by various amino peptidases resident in the cytosol or, alternatively, may escape from this attack by entering the endoplasmic reticulum (ER) by the transporter associated with antigen presentation (TAP). To study the possible consequences of this scenario for the efficiency of antigen presentation we have applied kinetic modelling. The mathematical model comprises the generation of primary oligomeric fragments containing the definitive epitope, the successive N-terminal shortening of these primary fragments by cytosolic amino peptidases and the TAP-mediated transport of cytosolic peptides into the ER. Because the number of peptide molecules may become very small we have performed deterministic and stochastic simulations of the kinetic model. Our simulations show that cytosolic N-terminal trimming of primary fragments may drastically increase loading epitope precursors into the ER. In particular, a primary fragment generated with a low rate of TAP transport into the ER may nevertheless become a potent epitope precursor if at least one of its N-terminal trimming products will be efficiently transported.

Keywords: MHC-1 presentation pathway, proteasome, TAP, epitope, kinetic modelling

1 Introduction

Cytotoxic T-cells of the vertebrate immune system are able to discriminate between ‘normal’ and ‘abnormal’ cells (exhibiting altered gene expression e.g. due to a viral infection) on the basis of the repertoire of peptides (T-cell epitopes) presented on the cell surface by the major histocompatibility complex class I (MHC-I). Before being presented at the cell surface, the epitope or a longer precursor peptide containing the epitope has to pass a number of consecutive filtering processes forming together the MHC-I presentation pathway (see [8] for a recent review). Most of the MHC-I presented peptides derived from oligomeric fragments generated by proteasomes from the pool of endogenous proteins. These primary fragments are either attacked by cytosolic proteases [1] or transported into the endoplasmic reticulum (ER) by the transporter associated with antigen presentation (TAP). Within the ER, peptides may undergo N-terminal trimming catalysed by a recently identified amino peptidase associated with antigen processing (ERAP) [10]. After proteasomal generation the C-terminus of peptides is not attacked by carboxy peptidases as demonstrated in experiments showing N-terminally

protected peptides to be stable [7]. Peptides with correct size and proper amino acid sequence motifs bind to MHC-I, and the receptor-peptide complex is transferred to the cell surface. Peptides in the ER with less efficient MHC-I binding are rapidly degraded.

Although meanwhile various cytosolic amino peptidases have been defined, the role of post-proteasomal cytosolic proteolysis for antigen presentation is still unclear. The common view is that cytosolic peptidases and ER peptidases act as epitope destructors accounting for the low efficiency of peptide presentation (only about one peptide out of every 10,000 proteins degraded will be presented by MHC class I molecules) [9]. However, computer-based discrimination between true MHC-1 ligands and random peptides on the sole basis of their TAP transport efficiencies significantly improve if transport of N-terminally extended epitope precursors is explicitly considered [3]. Thus, one may think of cytosolic proteases as a means to enlarge by partial hydrolysis the spectrum of fragments generated by proteasomes, thereby increasing the probability for the occurrence of epitope precursors in the cytosol that can be efficiently transported into the ER. To test this hypothesis in quantitative terms, we have established a kinetic model describing the cytosolic part of the MHC-1 presentation pathway: Generation of primary fragments the N-terminus of which may be further processed by cytosolic amino peptidases while each peptide may escape from further processing by transport into the ER. As the effective number of peptide molecules present in the cytosol may become very small if the generation of primary fragments proceeds with a low rate, we have performed not only deterministic but also stochastic simulations of the model. These calculations show that N-terminal trimming of longer primary fragments by cytosolic amino peptidases may result in peptides that can be very efficiently transported by TAP and thus increase the abundance of epitope precursors in the ER.

2 Method and Results

Mathematical Model

The reaction scheme of the kinetic model is shown in Fig. 1. $X(1, L)$ designates any primary peptide of length $L \geq L_0$ containing an epitope $X(L - L_0 + 1, L)$ of length L_0 between sequence positions $(L - L_0 + 1)$ and (L) . $X(1, L)$ is generated by the proteasome (or any other protease capable of cleaving full-size proteins) with rate v_g . This fragment as well as all other fragments $X(i, L)$ may be either attacked by cytosolic proteases with rates $k_p(i)$ or, alternatively, transported into the ER by TAP with rates $k_t(i)$. Several amino peptidases are known to work in the cytosol. However, their specific substrate preferences and activity levels are not known yet. In the model the combined effect of these peptidases on any peptide consists in splitting off the N-terminal residue with rate $k_c(i)$ thus reducing its size by one residue. The assumption of a consecutive 1-residue shortening of peptides is supported by experiments with peptides carrying fluorescent labels at various sequence positions. After injection into the cytosol the life times of peptides increases with ascending distance of the fluorescence label from the N-terminus. After $(L - L_0)$ successive N-terminal cleavages fragment $X(1, L)$ has been transformed into the definitive epitope $X(L - L_0 + 1, L)$. Peptides originating from further cleavage of $X(L - L_0 + 1, L)$ do not contain the full epitope sequence whereas all intermediates $X(1, L)$, $X(2, L)$, \dots , $X(L - L_0 + 1, L)$ represent epitope precursors which after uptake into the ER and further N-terminal trimming may contribute to the pool of epitopes presented on the cell surface.

To quantify the efficiency with which the epitope precursors enter the ER before being destroyed by the cytosolic proteases we define the *salvage efficiency* by summing up the TAP transport rates of all epitope precursors and referring this total rate to the generation rate v_g ,

$$\eta = \frac{1}{v_g} \sum_{i=1}^{L-L_0+1} k_t(i)X(i, L) \quad (1)$$

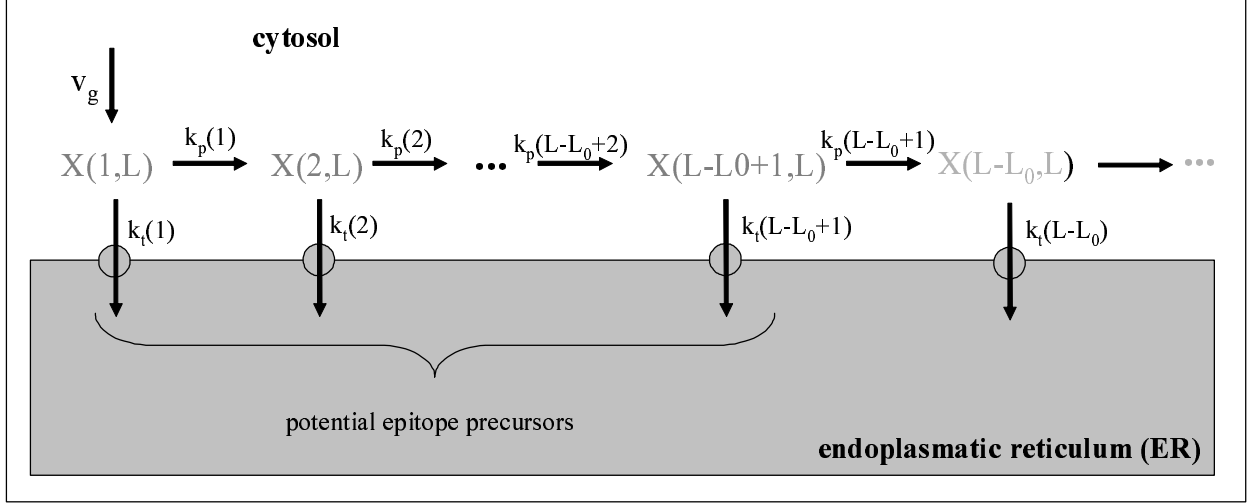


Figure 1: Reaction scheme for the cytosolic part of the MHC-1 presentation pathway.

The deterministic kinetic equations associated with the reaction scheme in Fig. 1 read

$$\begin{aligned} \frac{d[X(1, L)]}{dt} &= v_g - (k_p(1) + k_t(1)) [X(1, L)] \\ \frac{d[X(i, L)]}{dt} &= k_p(i-1)[X(i-1, L)] - (k_p(i) + k_t(i)) [X_i] \quad (i = 2, \dots, L - L_0 + 1) \end{aligned} \quad (2)$$

with $[X]$ designating the concentration of peptide X . For the stationary solution of system (1) we get

$$X(i, L) = \frac{v_g}{k_p(i)} \prod_{j=1}^i \frac{k_p(j)}{k_p(j) + k_t(j)} \quad (3)$$

Thus the salvage efficiency (1) is given by

$$\eta = \sum_{i=1}^{L-L_0+1} \gamma(i) \prod_{j=1}^i \frac{1}{1 + \gamma(j)} \quad (4)$$

with

$$\gamma(i) = \frac{k_t(i)}{k_p(i)} \quad (5)$$

relating the rate with which peptide $X(i, L)$ is transported into the ER to the rate of its proteolytic degradation.

For the formulation of the stochastic equations governing the above reaction scheme, we introduce the density function $P(n_L, n_{L-1}, \dots, n_{L-L_0+1}; t)$ representing the probability to find at time t in the cytosol n_1 molecules of peptide $X(1, L)$, n_2 molecules of peptide $X(2, L), \dots, n_{L-L_0+1}$ molecules of peptide $X(L - L_0 + 1, L)$. The time evolution of the density function can be described by the Master

equation

$$\begin{aligned}
\frac{d}{dt}P(n_1, \dots, n_{L-L_0+1}) = & \\
& v_g P(n_1 - 1, \dots, n_{L-L_0+1}) - k_p(1)n_1 P(n_1, \dots, n_{L-L_0+1}) \\
& + \sum_{i=2}^{L-L_0+1} [k_p(i-1)(n_{i-1} + 1)P(n_1, \dots, n_{i-1} + 1, \dots, n_{L-L_0+1}) \\
& \quad - k_p(i)n_i P(n_1, \dots, n_i, n_{i+1} - 1, \dots, n_{L-L_0+1})] \\
& + \sum_{i=1}^{L-L_0+1} [k_t(i)(n_i + 1)P(n_1, \dots, n_i + 1, \dots, n_{L-L_0+1}) - k_t(i)n_i P(n_1, \dots, n_i, \dots, n_{L-L_0+1})]
\end{aligned} \tag{6}$$

Numerical simulations of this equation for a physiologically relevant example are given below. Note that the concentration of a peptide is defined as expectation value of the corresponding particle number,

$$[X(i, L)] = \langle n_i \rangle = \sum_{n_1=1}^{\infty} \dots \sum_{n_{L-L_0+1}=1}^{\infty} n_i P(n_1, \dots, n_{L-L_0+1}) \tag{7}$$

Carrying out the summations in expression (7) across the master equation (6) we arrive after appropriate re-arrangements of summation indices at the deterministic equations (2).

Results

The Salvage Efficiency Increases with Increasing Size of Epitope Precursors

According to equation (4) the salvage efficiency decreases with decreasing values of the parameter $\gamma(i)$, i.e. the higher the proteolytic activity relative to the TAP transport rate, the lower the chance of epitope precursors to arrive at the ER. However, the values $\gamma(i)$ are determined by the specific amino acid sequences of the peptides and thus are fixed for a given primary fragment excised from the protein. Then, taking the salvage efficiency for the definitive epitope as the reference value, it follows from equation (4) that the generation of N-terminally extended precursors will always result in an increase of the salvage efficiency. This is illustrated in Fig. 2 for a peptide with length $L = L_0 + 1$, i.e. consisting of the epitope and carrying one additional residue at the N-terminus.

At fixed value of $\gamma_{epitope}$ the salvage efficiency increases with $\gamma_{precursor}$. If the TAP transport efficiency for the epitope is low compared with the rate of its proteolytic degradation (say $\gamma_{epitope} = 0.1$) whereas the TAP transport efficiency of the precursor is high compared with the rate of its proteolytic degradation (say $\gamma_{precursor} = 10$), the gain in the salvage efficiency amounts to about 10! More general, one may conclude that if at least one of the precursor peptides $X(1, L)$, $X(2, L)$, \dots , $X(L-L_0+1, L)$ formed along the cytosolic degradation route can be rapidly taken up into the ER before being further truncated, the salvage efficiency tends towards its maximum value.

Under Stationary Conditions the Variances of Cytosolic Peptide Numbers Equals Their Expectation Values

For the second momentum $\langle n_i^2 \rangle$ of the particle numbers one may derive the differential equation

$$\left. \frac{d}{dt} \langle n_i^2 \rangle \right|_{i>1} = (k_p(i) + k_t(i, L)) \langle n_i \rangle - 2(k_p(i) + k_t(i, L)) \langle n_i^2 \rangle + k_p(i-1) \langle n_{i-1} \rangle + 2k_p(i-1) \langle n_i n_{i-1} \rangle \tag{8}$$

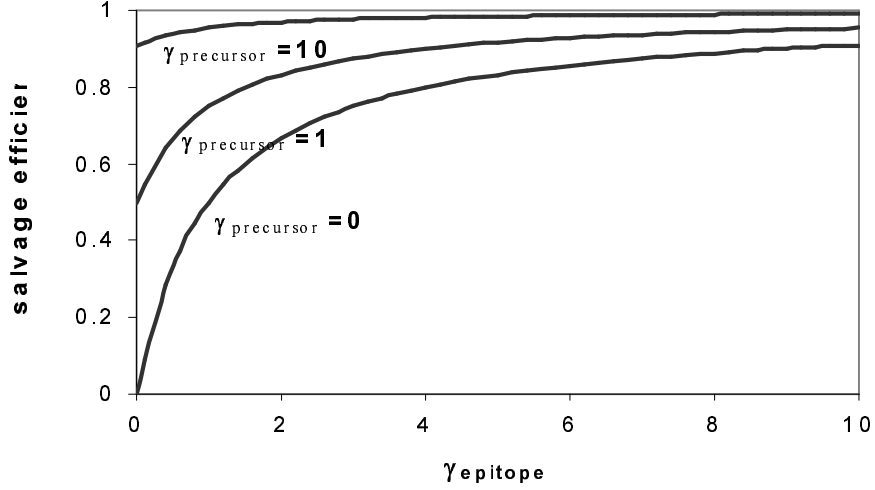


Figure 2: Salvage efficiency $\eta = \frac{1}{1 + \gamma_{precursor}} \left[\gamma_{precursor} + \frac{\gamma_{epitope}}{1 + \gamma_{epitope}} \right]$ the special case $L = L_0 + 1$; for the $\gamma_{precursor}$ and $\gamma_{epitope}$ represent the ratio between proteolytic rate and transport rate for the precursor $X(1, L)$ and the definitive epitope $X(2, L)$.

Under stationary conditions it follows that

$$\langle n_i^2 \rangle |_{i>1} = \frac{[k_p(i) + k_t(i)] \langle n_i \rangle + k_p(i-1) \langle n_{i-1} \rangle + 2k_p(i-1) \langle n_i n_{i-1} \rangle}{2[k_p(i) + k_t(i)]} = \langle n_i \rangle + \frac{\langle n_i n_{i-1} \rangle}{\langle n_{i-1} \rangle} \quad (9)$$

Replacing in this equation $\langle n_i \rangle = [X(i, L)]$ by the stationary solution of (2) we get for the variances

$$var(n_i) = \langle n_i^2 \rangle - \langle n_i \rangle^2 = \langle n_i \rangle \left[1 - \langle n_i \rangle + \frac{\langle n_i n_{i-1} \rangle}{\langle n_{i-1} \rangle} \right] = \langle n_i \rangle \quad (10)$$

The expression within the bracket reduces to unity because the covariances disappear in the stationary state, i.e. $\langle n_i n_j \rangle = \langle n_i \rangle \langle n_j \rangle$ for $i \neq j$. According to (10), the variance of the peptide number equals its expectation value. The magnitude of the random fluctuations of the peptide numbers around their expectation value is usually measured in terms of the coefficient of variation,

$$CoefVar(n_i) = \frac{\sqrt{Var(n_i)}}{\langle n_i \rangle} = \frac{1}{\sqrt{\langle n_i \rangle}} \quad (11)$$

The coefficient of variation (11) tends to zero for large peptide numbers but, on the other hand, tends to unity for very small peptide numbers. Hence one may expect large fluctuations of the peptide numbers for peptides present with low copy numbers.

Numerical Solutions of the Model for a Physiologically Relevant Example

Stochastic simulations of the kinetic model described above were performed using a 25mer of the viral pp89 protein as a model peptide. This 25mer (RLMYDMYPHFMPNTNLGPSEKRVWMS) contains a naturally processed epitope (YPHFMPNTNL) [2]. Proteasomal cleavage probabilities for the individual peptide bonds of the 25mer have been determined [4]. The absolute turnover rate of the proteasome was chosen such that 200 peptides per minute are generated from the pp89 25mer per. This rate corresponds to experimentally determined average digestion rates of proteins present in the cytosol

with medium concentration [6]. Random cleavages of the individual peptide bonds were treated as independent from each other. All fragments generated by two independent cuts were added to the cytosolic pool of peptides. Depletion of the pp89 25mer over the time period of the simulations was not considered.

For the computation of the TAP transport rates $k_t(i)$ we have used a recently proposed statistical model [3] that assigns a position-dependent transport score to the three N-terminal residues and the C-terminal residue of the peptide and combines these individual scores linearly to the total transport score. Peptides shorter than seven residues are not transported into the ER. Moreover, saturation of TAP transport capacity is not taken into account.

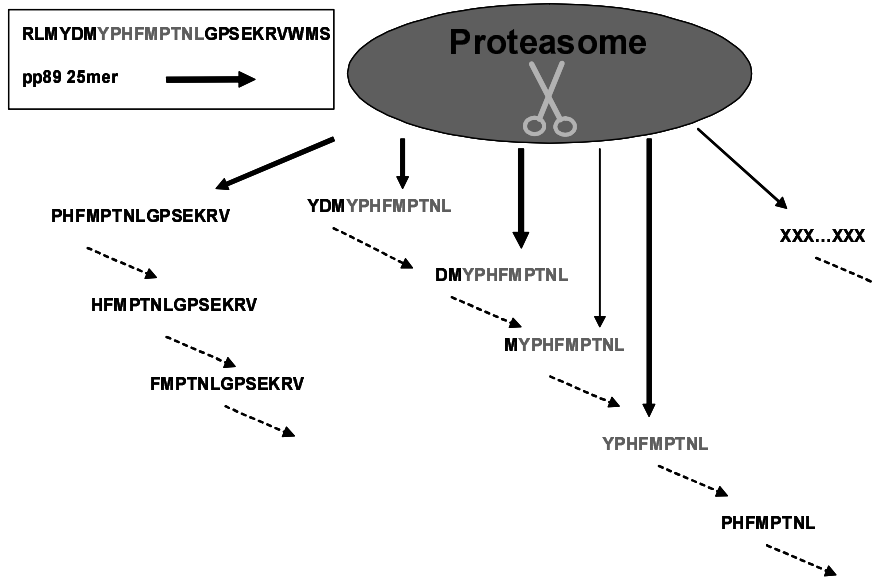


Figure 3: Proteasomal generation of primary fragments from the pp89 25mer. The proteasome digests the pp89 25mer and generates different peptide fragments (green solid arrows) with different efficiencies indicated by the arrow width. These peptides get gradually degraded by amino peptidases in the cytosol (black broken arrows). The naturally presented epitope is marked in light grey.

All peptides entering the ER via TAP transport and possessing the epitope (YPHFMPPTNL) were counted as potential epitope precursors that may contribute to the amount of epitopes presented on the cell surface. The rate constants $k_p(i)$ for the secession of the N-terminal residue are shown in Table 1. As no experimental data are available, we have studied 6 different hypothetical scenarios: (1) the rate constants are equal ($= 8 \text{ min}^{-1}$) for all possible N-terminal residues, (2) – (4): randomly chosen rate constants that are log-normally distributed with mean and deviance of 1.0., (5) rapid degradation of N-extended precursors but slow degradation of the epitope, (6) slow degradation of N-extended precursors but rapid degradation of the epitope.

Numerical simulations of the Master equation were carried out using the Gillespie algorithm. The simulation time was sufficiently long to study transient states as well as stationary states of the system.

The scattergrams in Fig. 4 illustrate how loading of peptides into the ER may vary depending on the residue specific rate constants of the amino peptidases. For comparison, in panels (a)-(c) the uptake rates ($=$ number of peptides transported into the ER per minute) computed by using the random sets (2) – (4) of cytosolic rate constants are plotted versus uptake rates obtained by using set (1) where all peptides are cleaved with the same rate. Notably, uptake rates may differ up to ten fold although the mean value of the rate constants for the various data sets in Table 1 is similar. The explanation is that those peptides that are only weakly attacked by the amino peptidases may accumulate in the cytosol and thus are transported into the ER with high rates. On the other hand, peptides degraded in the cytosol with high rates have little chance to escape into the ER. The large

Table 1: Different sets of cytosolic cleavage rate constants. Values are given in min^{-1} .

| N-terminal residue | (1) equal | (2) random | (3) random | (4) random | (5) e-save | (6) p-save |
|--------------------|-----------|------------|------------|------------|------------|------------|
| A | 8.00 | 175.54 | 6.68 | 6.91 | 8.00 | 8.00 |
| C | 8.00 | 64.45 | 0.07 | 429.65 | 8.00 | 8.00 |
| D | 8.00 | 0.12 | 76.80 | 0.36 | 40.00 | 0.20 |
| E | 8.00 | 0.05 | 1.16 | 0.98 | 8.00 | 8.00 |
| F | 8.00 | 0.17 | 1.76 | 0.58 | 8.00 | 8.00 |
| G | 8.00 | 31.53 | 69.77 | 2.26 | 8.00 | 8.00 |
| H | 8.00 | 11.59 | 3.93 | 1.72 | 8.00 | 8.00 |
| I | 8.00 | 0.31 | 0.48 | 0.13 | 8.00 | 8.00 |
| K | 8.00 | 14.67 | 0.66 | 0.59 | 8.00 | 8.00 |
| L | 8.00 | 0.28 | 2.20 | 0.48 | 40.00 | 0.20 |
| M | 8.00 | 0.24 | 0.17 | 0.02 | 40.00 | 0.20 |
| N | 8.00 | 0.04 | 3.82 | 0.80 | 8.00 | 8.00 |
| P | 8.00 | 0.35 | 1.15 | 4.08 | 8.00 | 8.00 |
| Q | 8.00 | 0.01 | 0.01 | 75.63 | 8.00 | 8.00 |
| R | 8.00 | 0.21 | 9.11 | 36.49 | 8.00 | 8.00 |
| S | 8.00 | 0.30 | 5.02 | 0.31 | 8.00 | 8.00 |
| T | 8.00 | 37.72 | 71.57 | 0.22 | 8.00 | 8.00 |
| V | 8.00 | 4.49 | 21.51 | 0.51 | 8.00 | 8.00 |
| W | 8.00 | 0.55 | 0.10 | 3.00 | 8.00 | 8.00 |
| Y | 8.00 | 0.37 | 0.56 | 6.63 | 0.01 | 800.00 |

impact of cytosolic cleavage rates on the efficiency of peptide precursor loading into the ER becomes even more transparent in Fig. 2d relating peptide amounts in the ER for the two extreme cases where the cytosolic proteases either rapidly degrade all N-extended epitope precursors whilst saving the definitive epitope, or vice versa.

In the further part of this work the set of equal rate constants (1) is used for cytosolic degradation due to lack of experimental data.

Representation of a sufficiently high amount of virus-specific epitopes on the surface of an infected cell is a prerequisite for initiating the attack of the cell by cytotoxic T-cells before new viruses have assembled and may leave the cell to infect other cells. Therefore, the time course of epitope production immediately after onset of protein synthesis is of great importance for preventing escalation of the virus infection. To study the impact of cytosolic proteases on the initial time-courses of epitope production we have performed stochastic simulations of the kinetic model for the pp89 system described above. Stochastic trajectories of all cytosolic peptides were computed over 30 minutes after onset of pp89 25mer degradation. Fig. 5 shows for the epitope and the three N-extended epitope precursors the number of copies generated within 30 minutes by the proteasome (Fig. 5a) and loaded into the ER (Fig. 5c). The epitope 7-15 (YPHFMPPTNL) and the three residues longer precursor 4-15 (YD-MYPHFMPPTNL) are generated with medium rates, whereas the precursor 5-15 (DMYPHFMPPTNL) is generated in higher quantity and the precursor 6-15 (MYPHFMPPTNL) is generated to a very small extend. The Poisson-like distributions of cytosolic copy numbers for these four peptides recorded during 30 minutes of simulation are depicted in Fig. 5b. Remarkably, the copy numbers of the 6-15 peptide (MYPHFMPPTNL) - although generated by the proteasome with very low efficiency - are of the same order as the copy numbers of the 5-15 or 7-15 peptide whereas the 4-15 precursor is present with the lowest copy numbers. This example demonstrates that striking differences may exist between the level of cytosolic copy numbers of a peptide and its proteasomal generation rate. Inspecting the efficiency of peptide loading into the ER, we note that only very few molecules of the 4-15 and 7-15

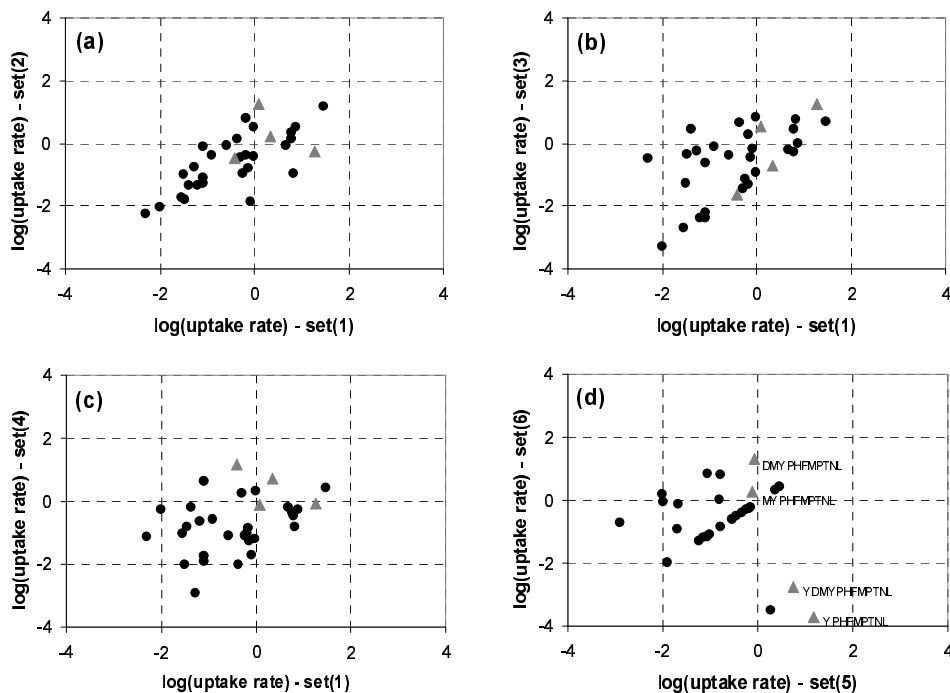


Figure 4: Variability of stationary peptide amounts in the ER for the different sets of rate constants for cytosolic amino peptidases given in Table 1. The (red) triangles mark the epitope and the three epitope precursors.

peptides but a large number of the 5-15 and 6-15 peptides get transported into the ER (Fig. 5c). This shows that a peptide occurring in proteasomal *in vitro* digests with very low abundance close to the threshold of the detection level can nevertheless be of great importance for antigen processing because of downstream processing in the cytosol. The example studied here illustrates a situation where the amount of an epitope peptide taken up into the ER during a 30 minutes time span would not suffice to trigger an immune response. Only the generation of N-extended precursor peptides by the proteasome - even if generated with small rates - raise the amount of potential epitopes in the ER to a level that is sufficient to stimulate cytotoxic T-cells.

Stochastic simulations are useful to assess variability of copy numbers. Owing to the stochastic nature of the elementary steps involved in antigen presentation individual cells will differ in the number of epitopes transported to the cell surface within a given time period. To explore the variability in the number of presented peptides we have performed 1000 simulations of the 30 minutes transient period after onset of peptide generation from the pp89 25mer. Fig. 6 shows the distribution of the copy numbers of the four potential antigenic sequences that have encountered the ER after 30 minutes. It is obvious that the epitope sequence itself is not able to activate an immune response since the number of peptides in the ER is astonishingly low; a significant number of cells (10%) have no epitope peptide in the ER at all. Relying on the epitope alone, these cells would not be able to trigger an immune response and therefore would represent a threat to the organism since the virus is able to replicate and infect new cells. On the other hand, two precursor epitopes are loaded into the ER with high copy numbers (see Fig. 6a). The total amount of peptides containing the epitope in the ER was larger than 200 in all 1000 simulations. Given that 10% of these precursors actually contribute to the pool of presented epitopes a surface loading of 20 peptides can be expected that should be sufficient to trigger an immune response. This example underlines again the importance of epitope precursors for the increasing the efficiency of antigen presentation.

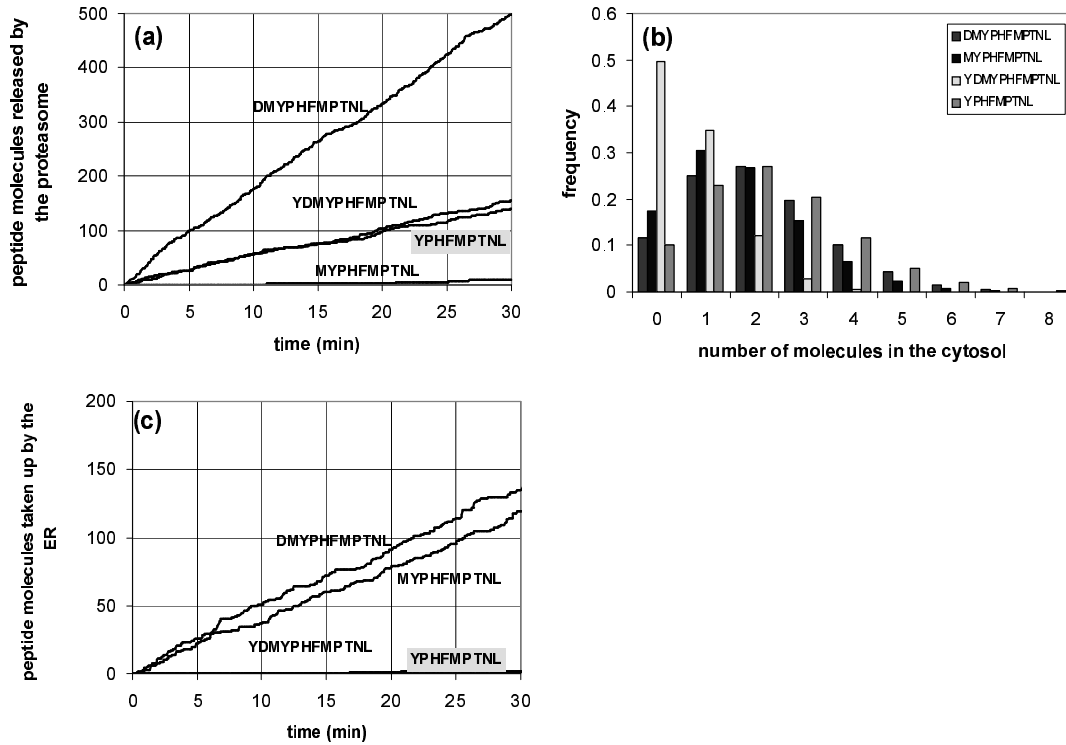


Figure 5: Simulated stochastic time courses of the four epitope precursors excised from the pp89 25mer. (a) Number of peptides generated by the proteasome. (b) Histogram of cytosolic peptide numbers. (c) Number of peptides taken up into the ER.

3 Discussion

In this work we have proposed a kinetic model to study the consequences of post-proteasomal proteolytic peptide processing in the cytosol for the efficiency of antigen presentation. Our calculations demonstrate that in the presence of cytosolic trimming processes, all precursors of a potential epitope may ultimately serve as a valuable source of antigen presentation irrespective of these precursors being directly generated by the proteasome or indirectly by cytosolic amino peptidases. In contrast to the common view, cytosolic N-terminal trimming of primary fragments does not necessarily lower the yield of presented epitopes but instead may significantly increase it. Our results indicate that there is no simple 1:1 relationship between the rate with which the definitive epitope is generated by the proteasome (typically assessed in an *in vitro* assay) and the efficiency with which this epitope will be presented. Under extreme conditions N-extended epitope precursors either generated by the proteasome or /and by the action of amino peptidases in the cytosol and the ER may represent the sole source of antigens.

It has to be noted, however, that our computational studies were restricted to a certain section of the whole MHC-1 presentation pathway ending with the uptake of peptides into the ER. Whether or not N-extended epitope precursors actually will contribute to the pool of presented epitopes depends essentially upon the efficiency of the succeeding steps, i.e. binding to the MHC-1 molecule complex and excision of the N-terminal extension by amino peptidases of the ER.

In the pp89 simulations we have used physiologically meaningful values of the model parameters for the proteasomal generation of primary fragments and the transport of peptides into the ER. From the simulation results it can be inferred that certain peptides may occur in the cytosol and in the ER with very low copy numbers. Hence, mathematical modeling of the MHC-1 presentation pathway has to include stochastic computations to estimate the variability of presented epitopes among individual

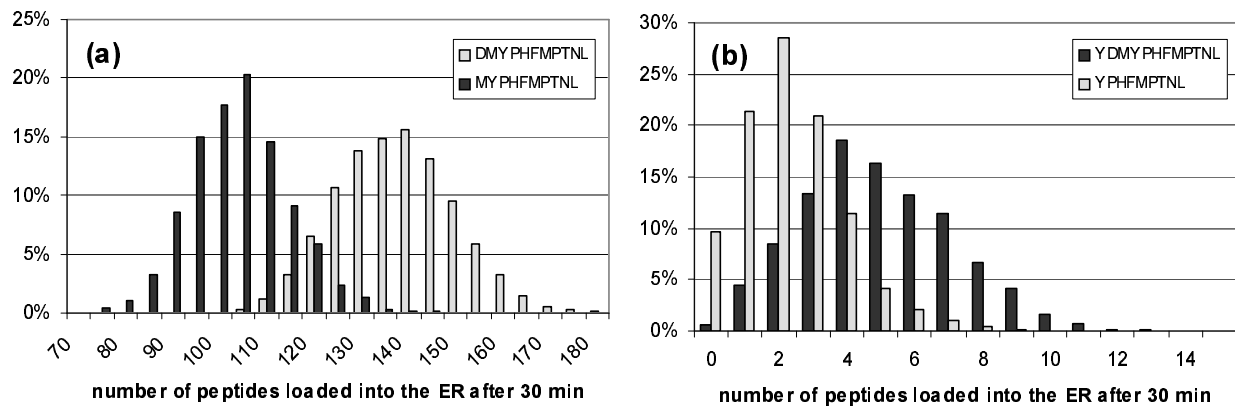


Figure 6: Distribution of peptide copies that have entered the ER after 30 minutes. The distributions are based on 1000 stochastic simulations. (a) Low abundant epitope precursors. (b) High abundant epitope precursors.

cells.

The presented computations in this article are part of our long-term effort to set up a reliable kinetic model of the whole MHC-1 presentations pathway. Since this biochemical system is very complex and not all features can be measured *in vivo* we have decided to follow a “divide et impera” approach by dissecting the whole pathway into smaller functional units that are being experimentally studied and modeled separately and will finally be reassembled. The progress of this strategy is mostly limited by the availability of consistent and high-quality kinetic data required for the estimation of numerical values for model parameters. This condition is currently met for the peptide binding to certain MHC-1 alleles [5] and the TAP transporter [3]. The existing algorithms for the computer-based prediction of proteasomal cleavages are less reliable (for a comparison of these algorithms see [3]). For the amino peptidases in the cytosol and in the ER experimental data allowing for the estimation of sequence-specific rate constants are completely lacking. However, as shown here by simulations based on different sets of arbitrarily chosen rate constants for the cytosolic trimming proteases (cf. Fig. 4) knowledge of the kinetic properties of these proteases will be essential for improving the physiological reliability of the proposed model. Knowledge of these rates is also essential to benefit from an improved prediction of proteasomal cleavages: currently only cleavage of the C-terminus can be used to identify potential epitopes, as the C-terminus is shared by the epitope and all its precursors. Any attempt to use the information which N-termini are generated by the proteasome can only improve epitope identification when it is known how these fragments are trimmed in the cytosol and the ER.

References

- [1] Herberts, C., Reits, E., and Neefjes, J., Proteases, proteases and proteases for presentation, *Nat. Immunol.*, 4:306–308, 2003.
- [2] Knuehl, C., Spee, P., Ruppert, T., Kuckelkorn, U., Henklein, P., Neefjes, J., and Kloetzel, P.M., The murine cytomegalovirus pp89 immunodominant H-2Ld epitope is generated and translocated into the endoplasmic reticulum as an 11-mer precursor peptide, *J. Immunol.*, 167:1515–1521, 2001.
- [3] Peters, B., Bulik, S., Tampe, R., van Endert, P.M., and Holzhutter, H.G., Identifying MHC class I epitopes by predicting the TAP transporter efficiency of epitope precursors, *J. Immunol.*, 171:1741–1749, 2003.

- [4] Peters, B., Janek, K., Kuckelkorn, U., and Holzhutter, H.G., Assessment of proteasomal cleavage probabilities from kinetic analysis of time-dependent product formation, *J. Mol. Biol.*, 318:847–862, 2002.
- [5] Peters, B., Tong, W., Sidney, J., Sette, A., and Weng, Z., Examining the independent binding assumption for binding of peptide epitopes to MHC-I molecules, *Bioinformatics*, 19:1765–1772, 2003.
- [6] Princiotta, M.F., Finzi, D., Qian, S.B., Gibbs, J., Schuchmann, S., Buttgereit, F., Bennink, J.R., and Yewdell, J.W., Quantitating protein synthesis, degradation, and endogenous antigen processing, *Immunity*, 18:343–354, 2003.
- [7] Reits, E., Griekspoor, A., Neijssen, J., Groothuis, T., Jalink, K., van Veelen, P., Janssen, H., Calafat, J., Drijfhout, J.W., and Neefjes, J., Peptide diffusion, protection, and degradation in nuclear and cytoplasmic compartments before antigen presentation by MHC class I, *Immunity*, 18:97–108, 2003.
- [8] Shastri, N., Schwab, S., and Serwold, T., Producing nature’s gene-chips: The generation of peptides for display by MHC class I molecules, *Annu. Rev. Immunol.*, 20:463–493, 2002.
- [9] Yewdell, J.W., Reits, E., and Neefjes, J., Making sense of mass destruction: quantitating MHC class I antigen presentation, *Nat. Rev. Immunol.*, 3:952–961, 2003.
- [10] York, I.A., Chang, S.C., Saric, T., Keys, J.A., Favreau, J.M., Goldberg, A.L., and Rock, K.L., The ER aminopeptidase ERAP1 enhances or limits antigen presentation by trimming epitopes to 8-9 residues, *Nat. Immunol.*, 3:1177–1184, 2002.